

A Density Functional Theory Investigation of Carboranethiol Self-Assembled Monolayer on Au(111)

Ersen Mete,^{*,†} Ayşen Yılmaz,[‡] and Mehmet Fatih Danışman^{*,‡}

*Department of Physics, Balıkesir University, Balıkesir 10145, Turkey, and Department of
Chemistry, Middle East Technical University, Ankara 06800, Turkey*

E-mail: emete@balikesir.edu.tr; danisman@metu.edu.tr

KEYWORDS: DFT Calculations, Carboranethiol, Self-Assembled Layers, Au Surface

^{*}To whom correspondence should be addressed

[†]Department of Physics, Balıkesir University, Balıkesir 10145, Turkey

[‡]Department of Chemistry, Middle East Technical University, Ankara 06800, Turkey

Abstract

Isolated and full monolayer adsorption of various carboranethiol ($C_2B_{10}H_{12}S$) isomers on gold (111) surface have been investigated using both the standard and van der Waals density functional theoretical calculations. The effect of differing molecular dipole moment orientations on the low energy adlayer geometries, the binding characteristics and the electronic properties of the self-assembled monolayers of these isomers have been studied. Specifically, the binding energy and work function changes associated with different molecules show a correlation with their dipole moments. The adsorption is favored for the isomers with dipole moments parallel to the surface. Of the two possible unit cell structures, the (5×5) was found to be more stable than the $(\sqrt{19} \times \sqrt{19})R23.4^\circ$ one.

Introduction

Thiol self-assembled monolayers (SAMs) on metal surfaces are ubiquitous systems due to their easy adaptability in many different applications ranging from bio-sensors to electronics.¹⁻⁴ The utility of these systems is that by designing/using an appropriate thiol molecule, the properties of the metal surfaces can be altered in a controlled way. The properties of thiol SAMs are governed by the balance between the intermolecular and molecule-surface interactions and have been the subject of intense experimental²⁻⁷ and computational⁸⁻³⁹ studies. By playing with the chemical nature of the thiol molecules this balance can be altered and SAMs with different structural, interface and/or surface properties could be obtained.

One very important property, especially for electronic applications, is the work function of the metal surface coated with the SAM which can be controlled by tuning the dipole moment of the molecules forming the SAM.^{18,20,21,30,31,34,40,41} To alter the work function either single component SAMs made up of thiol molecules with appropriate dipole moment or mixed SAMs made up of two different thiol molecules each with a different dipole moment can be employed.^{17,41-46} In both cases, most of the time, the dipole moment of the molecules are tuned by adding a functional group to the backbone or to the end of the molecules. This approach however not only changes the

dipole moment but also alters the geometry of the molecule which in turn may result in SAMs with different structural properties which is coupled to the electronic properties of the film/surface. To be able to study the effect of geometry and the chemical/electronic nature of the molecule on the properties of the film independently, hence, it is necessary to decouple these two changes in the molecule. Dicarbacloso-dodecaborane thiols ($C_2B_{10}H_{12}S$, will be referred to as carboranethiols) is an outstanding alternative to this end, since by playing with the positions of the carbon and sulfur atoms, the electronic properties of the molecule (i.e. dipole moment) can be altered without changing geometry. This fact combined with their chemical stability and almost spherical shape make CTs unique molecules for studying the fundamental properties of thiol SAMs and for preparing films that can be used in many different applications. Hence, SAMs of CTs and their derivatives have attracted increasing interest in recent years.^{47–58}

Recently, Lübben and coworkers have demonstrated that by using pure and mixed SAMs of two carborane dithiol isomers [1,2-(HS₂)-1,2- $C_2B_{10}H_{10}$ and 9,12-(HS₂)-1,2- $C_2B_{10}H_{10}$] with opposite dipole moments, the surface potential of silver surfaces could be tuned. Weiss et al., on the other hand, used two CT isomers [1-HS-1,7- $C_2B_{10}H_{11}$ (M1) and 9-HS-1,7- $C_2B_{10}H_{11}$ (M9), see figure 1 for naming of CT isomers] and were able to tune the gold work function over a range of 0.8 eV by preparing mixed SAMs of these two isomers in different ratios.⁵³ Then, they used such SAM coated gold surfaces as electrodes of organic field effect transistors and observed an improvement in the device characteristics. In addition they found that M1 adsorbs on the Au(111) surface stronger than M9, based on contact angle and reflection absorption IR spectroscopy results, and attributed this to dipole-dipole interactions of the molecules in the SAM. In case of M1 the dipole moment vector of the molecule is parallel to the gold surface (see Figures 1 and 2) whereas for M9 the direction is perpendicular to the surface. Hence Weiss *et al.* proposed that the head-to-tail orientation of the dipoles of the M1 molecules could yield a more favorable adsorption when compared with M9. In addition, very recently they showed that dipole-dipole interactions to be highly defect tolerant based on STM measurements⁵⁷ which can be interpreted as another outcome of the importance of the dipole-dipole interactions on determining thiol film structure and adsorption

strength. Finally, based on scanning tunneling microscope images, they suggested two possible unit cell $[(5 \times 5) \text{ and } (\sqrt{19} \times \sqrt{19})\text{R}23.4^\circ]$ structures for M1 and M9 SAMs which are depicted in Figure 3.⁵⁵

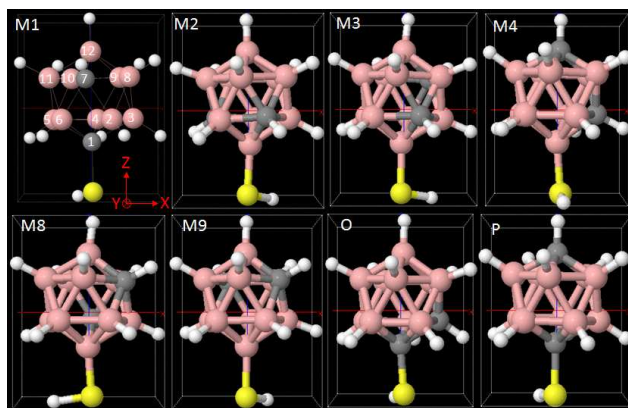


Figure 1: The vdW-optimized structures of CT isomers. The numbering scheme is given in the M1 molecule.

In order to describe the atomic and electronic structures of isolated and full monolayer adsorption of carboranethiols on the flat gold surface, periodic boundary density functional theory (DFT) calculations were carried out based on the projector augmented-wave (PAW)⁵⁹ method as implemented in VASP.^{60–62} Single particle valence states were expanded in terms of plane waves up to a kinetic energy cutoff of 400 eV. The electron-electron exchange and correlation interactions have

been included using both the standard Perdew-Burke-Ernzerhof (PBE) functional within the generalized gradient approximation (GGA) and the dispersion corrected optB86b-vdW functional⁶³ within the van der Waals density functional (vdW-DF) approach.⁶⁴ The vdW correction mimics the attractive electronic interactions beyond the equilibrium separations. Therefore, the basic idea is to include the long range part of the correlation energy as a fully nonlocal functional of the charge density.

Before moving on to the surface properties, we tested PBE and optB86b-vdW (exchange-correlation) XC functionals against the lattice parameter of the bulk gold (fcc). The standard PBE gives a value of 4.160 Å. The vdW correction leads to 4.125 Å which better compares with the experimental value of 4.078 Å.⁶⁵ We modeled the flat gold surface as a four atomic layer slab in a supercell which also contains a vacuum region with a height of 21 Å along the surface normal. This vacuum separation reduces to 14 Å after CT molecule adsorption on the surface. Initial coordinates of gold atoms were taken from their bulk positions. Then, we performed a full optimization of the ionic coordinates and lattice translation vectors based on the variational minimization of the Hellmann-Feynman forces by requiring each spatial component to be less than 0.01 eV/Å on each atom. The average nearest neighbor Au-Au bonds were found as 2.917 Å with and as 2.942 Å without the dispersive corrections. The standard XC functionals tend to overestimate the bond lengths especially in metallic systems. This is basically due to the local density approximation (LDA). It tries to parametrize the XC energy as a functional of the electron density from the uniform distribution of an homogeneous electron gas with the same charge density.

For calculations involving molecular adsorbates on the surface, the gold atoms at the bottom two layers were frozen to their fully relaxed positions. The (5×5) surface unit cell is considered for the adsorption of an isolated CT on Au(111). This supercell is large enough to put at least 9.9 Å separation between the periodic images of the CT adsorbates on the surface.

In the full monolayer CT coverage on flat gold, we considered the (5×5) and $(\sqrt{19} \times \sqrt{19})R23.4^\circ$ structures as a probable surface phases as suggested by recent experiments.⁵⁵ The surface Brillouin zone integrations were carried out over k -point samplings with Γ -centered $5 \times 5 \times 1$ meshes. Our

tests with denser k -point grids showed that the total energies were converged to an accuracy of 10 meV. The density of states (DOS) calculations were performed with $7 \times 7 \times 1$ k -point mesh using the tetrahedron method.

The dissociative adsorption energies of Au(111) surfaces with isolated and full monolayer CTs can be calculated by,

$$E_{\text{ads}} = E_{\text{CT/Au(111)}} - E_{\text{Au(111)}} - n(E_{\text{CT}} - \frac{1}{2}E_{\text{H}_2}),$$

where $E_{\text{CT-H/Au(111)}}$, $E_{\text{Au(111)}}$, E_{CT} and E_{H_2} are the total energies of the Au(111) slab with CTs which lost their tail hydrogens, of the clean Au(111) slab, of a single CT in a big box and of a hydrogen molecule in vacuum, respectively. In this expression, n is the number of CT adsorbates on the surface.

Table 1: Relative total energies, E_t , and dipole moments, μ , of carboranethiol (CT) compounds in the gas phase calculated using both PBE and optB86b-vdW functionals.

CT	PBE					vdW-DF				
	E_t	μ_x	μ_y	μ_z	μ	E_t	μ_x	μ_y	μ_z	μ
M1	0.999	-0.56	-1.55	-0.66	1.78	1.008	-0.58	-1.53	-0.64	1.76
M2	0.002	-0.41	-0.43	-1.53	1.64	0.013	-0.40	-0.43	-1.50	1.61
M3	0.020	3.08	0.05	0.81	3.18	0.040	3.05	0.05	0.77	3.15
M4	0.000	2.16	-0.40	2.29	3.17	0.000	2.13	-0.39	2.26	3.13
M8	0.008	1.59	1.21	0.84	2.16	0.018	1.58	1.20	0.82	2.15
M9	0.065	1.27	1.53	3.34	3.89	0.085	1.26	1.52	3.33	3.87
Ortho	1.576	1.78	0.96	-3.10	3.70	1.596	1.76	0.92	-3.08	3.66
Para	0.869	-0.25	0.59	0.84	1.06	0.887	-0.25	0.57	0.81	1.02

Results and Discussion

The gas phase structures of various CT variants were obtained with both the standard PBE and the modern vdW-DF functionals. The positional labeling of the carboranethiol isomers follow as shown in Figure 1. Although the cage geometries are essentially similar their relative total energies and dipole moments are different (see Table 1).

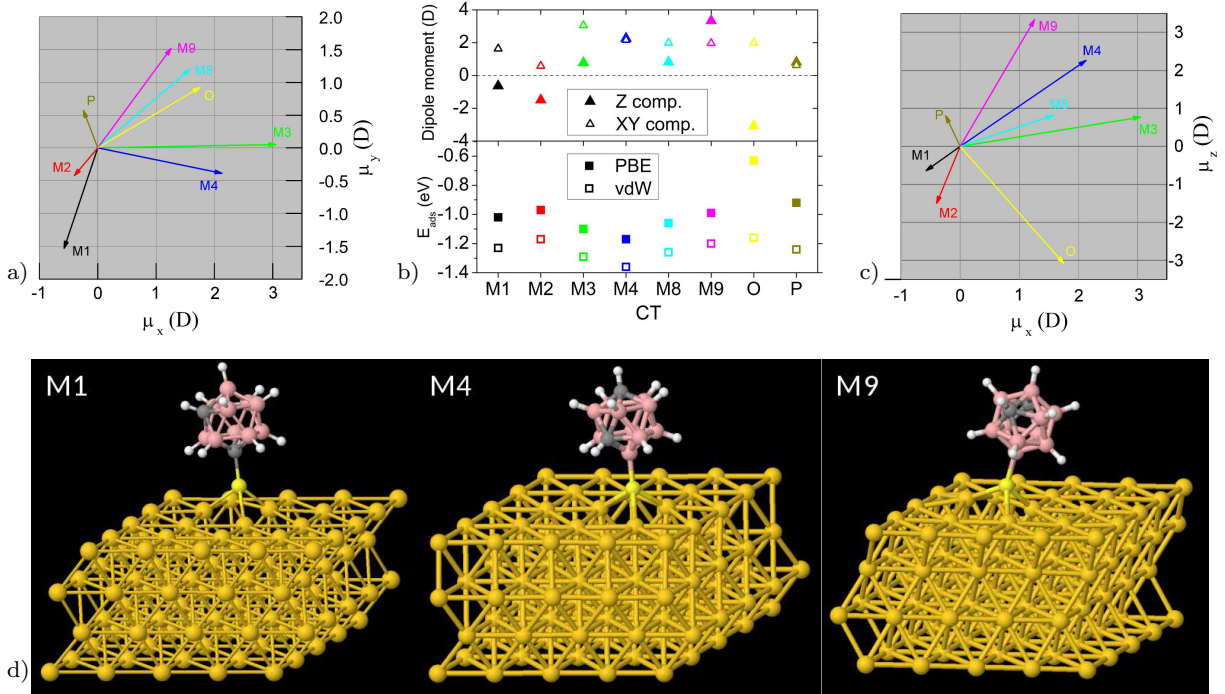


Figure 2: Plots showing the a) XY, c) XZ components of the dipole moments of the CT isomers in the gas phase. b) Chart showing the Z, XY components of the dipole moments and corresponding adsorption energies of CT isomers on Au(111). d) Optimized geometries of the isolated M1, M4 and M9 CTs on the gold surface.

We considered all probable adsorption configurations of CTs on the unreconstructed gold (111) surface. For instance, the adsorption of M9 on gold at the bridge site is energetically 0.52 eV higher than the most favorable position at the hollow site. In addition, when initially placed on top of one of the surface gold atoms, the molecule relaxes into the bridge configuration. We also checked and saw that a geometry optimization of an isolated CT starting from the bridge does not end up with the hollow position. This result is not enough to rule out the possibility of the coexistence of both adsorption types in an experimental realization. Indeed, our 1 ML results show that while most of the molecules are adsorbed at the hollow site, small number of them come close to the bridge site as shown in Figure 3.

Table 2: Relative total cell energies, E_t , and dissociative adsorption energies, E_{ads} , of Au(111) with a single isolated CT, calculated using PBE and optB86b-vdW methods.

CT	PBE				optB86b-vdW			
	E_t	E_{ads}	d_{S-Au}	h	E_t	E_{ads}	d_{S-Au}	h
M1	1.14	-1.02	2.44, 2.47, 2.57	1.49	1.15	-1.23	2.42, 2.44, 2.52	1.43
M2	0.21	-0.97	2.44, 2.46, 2.53	1.45	0.20	-1.17	2.42, 2.44, 2.48	1.37
M3	0.10	-1.10	2.45, 2.45, 2.51	1.51	0.10	-1.29	2.44, 2.45, 2.49	1.48
M4	0.00	-1.17	2.43, 2.45, 2.50	1.40	0.00	-1.36	2.39, 2.41, 2.46	1.35
M8	0.13	-1.06	2.43, 2.45, 2.51	1.41	0.11	-1.26	2.42, 2.43, 2.48	1.37
M9	0.24	-0.99	2.45, 2.46, 2.50	1.55	0.19	-1.20	2.43, 2.45, 2.49	1.51
Ortho	2.11	-0.63	2.43, 2.44, 2.51	1.44	1.79	-1.16	2.42, 2.43, 2.49	1.38
Para	1.12	-0.92	2.44, 2.47, 2.56	1.48	1.00	-1.24	2.41, 2.42, 2.49	1.35

In the minimum energy adsorption, a single CT molecule attaches to the surface via its tail sulphur which shows three-fold coordination with the nearest neighbor gold atoms at the hollow site. The three S-Au bonds are not equal in length as presented in Table 2. For the isolated case of M9 on Au(111), they are found as 2.45, 2.46, 2.50 Å with PBE and 2.43, 2.45, 2.49 Å with vdW-DF at the hollow position. Although the vdW-DF bond lengths are only slightly shorter than the PBE ones, the inclusion of the dispersive forces have non negligible effect on the minimum energy geometries especially on the surface gold atoms in the vicinity of the adsorption region. The standard PBE functional leads to considerable local distortion on the gold surface while it is less noticeable when vdW corrections apply. For instance, M9 sits on the hollow site above the

surface gold triangle where the three Au-Au distances become 3.45, 3.49, 3.49 and 3.37, 3.37, 3.42 Å with the PBE and optB86b-vdW functionals, respectively.

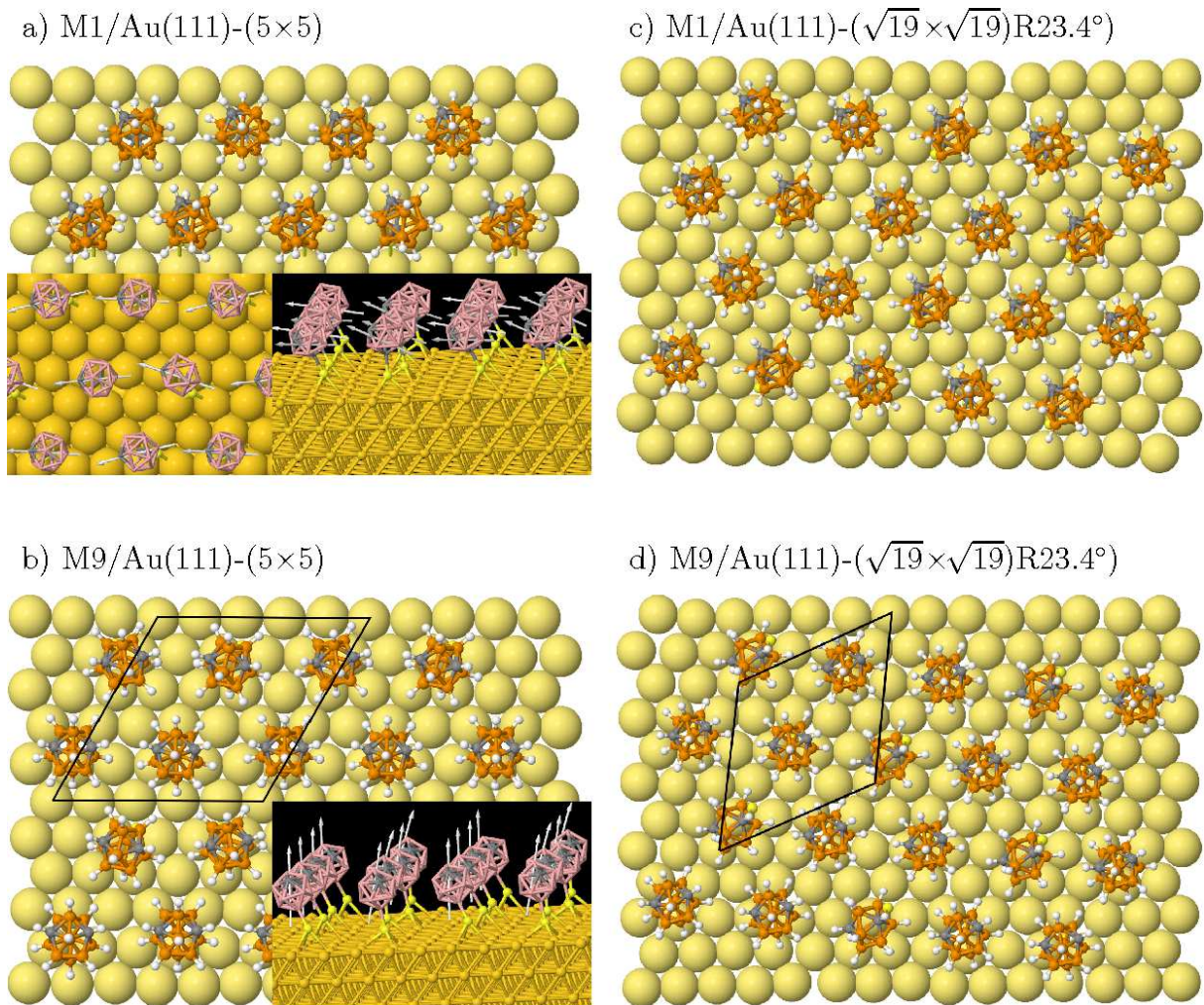


Figure 3: The adsorption geometry of (5×5) and $(\sqrt{19} \times \sqrt{19})$ R23.4° structures of 1ML M1 and M9 on the unreconstructed Au(111) surface optimized using vdW-DF.

In Figure 2, the dipole moments and the adsorption geometries of the studied CT isomers are shown. When the z components of the dipole moments are considered, a correlation with the adsorption energies can be noticed. A dipole moment vector pointing above the surface results in lower binding energies with both PBE and optB86b-vdW functionals. Whereas dipole moment vectors pointing towards the surface increase binding energies.

The work function of the clean gold (111) surface is calculated using the expression $W = V(\infty) - E_F$ as 5.15 eV. Here, $V(\infty)$ is the electrostatic potential in the vacuum and E_F is the Fermi

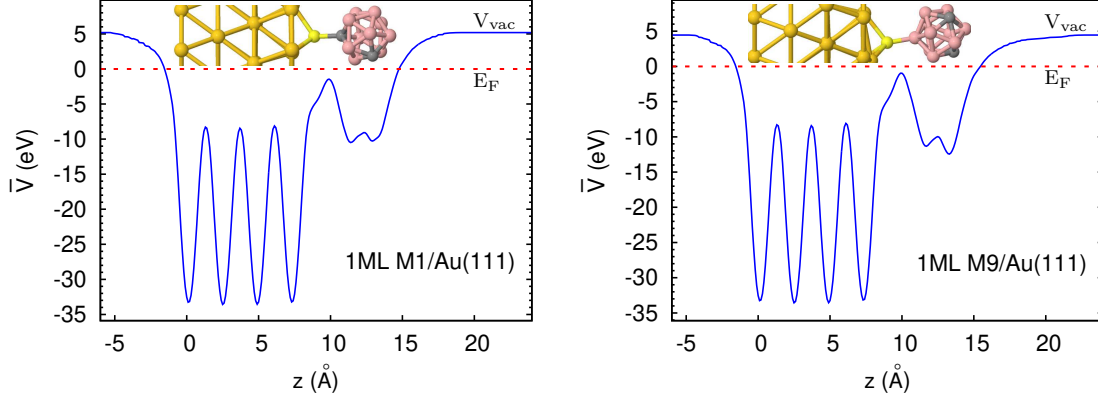


Figure 4: Electrostatic potential energy profiles of the Au(111) slab with M1 and M9 CT adlayers. $\bar{V}(z)$ is plane averaged along the surface normal. V_{vac} is the potential energy value at the vacuum regions and E_F is Fermi level.

energy. We obtained the real space electrostatic potential $V(x, y, z)$ in a self-consistent DFT calculation. Then the plane averaged potential is given by

$$\bar{V}(z) = \frac{1}{A} \iint_{\text{cell}} dx dy V(x, y, z) \quad (1)$$

where A is the surface unit cell area. The plots for surfaces with M1 and M9 SAM structures are presented in Figure 4.

The dissociative adsorption of an isolated M9 molecule on the gold (5×5) surface corresponding to 0.25 ML coverage yields a work function of 4.81 eV. The same surface structure with an isolated M1 gives this value as 5.13 eV. For a full M9 adlayer on the gold surface, it becomes 4.45 eV while M1 SAM leads to a work function of 5.20 eV. In other words, M9 SAM results in a reduction of 0.70 eV in the work function of the gold surface while M1 SAM increases it by 0.05 eV. When the electrostatic potential profiles of M1 and M9 SAM structures in Figure 4 are compared, the higher potential well depth of M1 indicates a lower electron density in the molecular film relative to M9. This implies a stronger interaction between the M1 layer and the gold surface. Therefore, these results indicate a better binding in favor of M1 adlayer. Weiss *et al.*, in their experimental study, have reported a reduction of 0.4 eV for M9 and increase of 0.4 eV for M1 SAMs.⁵³ Though the changes in the work function due to individual M1 and M9 SAMs we report

here do not match very well with the experimental results, the total variation (0.75 eV) agrees very well with the experimental value (0.8 eV).

Table 3: Relative total cell energies, E_t , the dissociative adsorption energies, E_{ads} , and the heights of a full CT adlayer on Au(111) with two different phases calculated using the PBE and the optB86b-vdW exchange-correlation functionals.

CT	PBE						optB86b-vdW					
	(5×5)			$(\sqrt{19}\times\sqrt{19})R23.4^\circ$			(5×5)			$(\sqrt{19}\times\sqrt{19})R23.4^\circ$		
	E_t	E_{ads}	h	E_t	E_{ads}	h	E_t	E_{ads}	h	E_t	E_{ads}	h
M1	3.55	-0.48	2.05	3.51	0.73	1.55	2.74	-0.70	2.02	2.44	-0.35	1.49
M9	0.00	-0.30	2.05	0.00	0.79	1.56	0.00	-0.51	2.01	0.00	-0.02	1.49

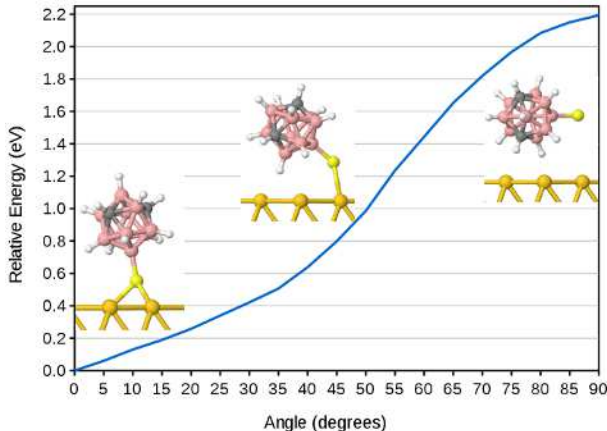


Figure 5: Relative energy of single M9 + Au(111) combined system with respect to the tilting angle of S-Au bond. The zero of the angle is set as the minimum energy vertical alignment of M9 that is not perfectly perpendicular to the surface.

We have computed the relative cell energy of an isolated M9 as a function of the tilting angle as shown in Fig. 5. M9 makes an angle of $\sim 10^\circ$ with the surface normal at its minimum energy binding. The potential energy barrier is almost 2.1 eV between standing up and lying parallel orientations. This big energy difference can be attributed to the generation of strong Au-S bonds by M9 with large molecular dipole.

The average value of the nearest neighbor spacings between the carboranethiol isomers at 1ML on Au(111)- (5×5) are about 7.2 Å and 7.0 Å with and without vdW corrections. The corresponding mean values slightly change to 7.4 Å and 7.2 Å on the $(\sqrt{19}\times\sqrt{19})R23.4^\circ$ structure. These

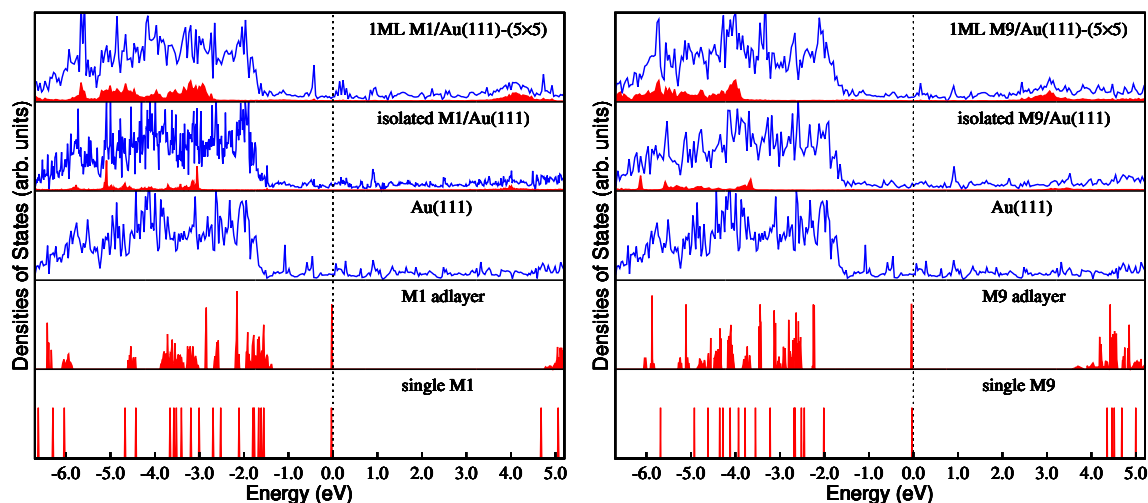


Figure 6: Calculated total and partial densities of states (DOS) of isolated and 1ML M1/M9 CT on Au(111). Shaded regions indicate the molecular contributions. The DOS plots of a single M1/M9 in the gas phase and of an adlayer without the gold slab are presented in the lower two panels, correspondingly.

geometry optimization results are consistent with experimental value of 7.2 ± 0.4 Å.⁵⁵ When the relative total energies of the flat gold surfaces with M1 and M9 adlayers are compared, the latter is found to be energetically more preferable than the former by 3.55 eV by PBE or 2.74 eV by vdW-DF per (5×5) unit cell as seen in Table 3. On the other hand, the adsorption energy comparisons favor M1 over M9 in terms of stability at both low and full concentrations. The PBE functional appears to underestimate the adsorption energies. Especially, PBE does not give any binding for 1 ML CT on $(\sqrt{19} \times \sqrt{19})R23.4^\circ$ unit cell yielding a positive adsorption energy. This result urges the importance of vdW corrections in the theoretical description of metal-organic systems. Hohman *et al.* reported that M1 is the preferred species in mixed monolayers. Our vdW-DF results indicate a stronger adsorption in favor of M1 relative to M9 in good agreement with the experiments.⁵⁵ The most striking difference of these similar CT isomers is their dipole moments. Therefore, the dipole-dipole interactions between the molecules has a significant role in the SAM stability on the gold surface.

We have calculated the total and projected densities of states (DOS) of Au(111) with M9 and M1 at low and full coverages using the vdW-DF theory calculations. We chose M9 and M1 because they cause work function changes in the opposite directions. We first stated with the electronic

structures of a single M9(M1) in the gas phase and of an M9(M1) adlayer without the gold slab as shown in the lower two panels of Fig. 6. The HOMO-LUMO separation of M9(M1) is found to be 4.4(4.7) eV. Due mostly to dipole-dipole interactions within the CT layers, the energy levels, in both cases, get slightly dispersed without showing a significant shift in their positions. The weakness of the coupling between the molecules show itself as a broadening of the energy levels mimicking a long-range correlation effect. The isolated and 1 ML M1 on Au(111) show similar characteristics. However, they differ from the M1 cases for which gold slab is absent. Due to the formation of strong Au-S bonds the DOS contributions of M1 species exhibit a significant red shift in the energy spectra of CT-Au(111) systems. Similar conclusions can be drawn for the M9 case. On the other hand, one can notice that M1 peak positions energetically lie lower relative to those of M9. Therefore, the binding characteristics of M1 is favored over M9. This result is also consistent with our calculated adsorption energies in Table 3. Although the dipole-dipole interactions are weak in SAMs, the inclusion of vdW correction terms in the description of electronic structures of organic-metal interfaces becomes important.

Conclusions

We carried out periodic density functional theory calculations by considering isolated and full adlayer of carboranethiol isomers on the Au(111) surface. In order to quantitatively show the effect of the long-range correlations on both the final geometries of CT-metal composite systems and their electronic structures, we included dispersive forces in a self-consistent implementation of the vdW-DF method. Then comparisons were made with the results obtained using the standard exchange-correlation functional.

Isolated carboranethiols prefer the hollow site for dissociative adsorption on the gold (111) surface by forming strong Au-S bonds. PBE calculations indicate that M4 has the lowest total energy among the other isomers in the gas phase. M1 has a dipole moment almost parallel to the surface while M9 has a moment nominally along the surface normal. Their 1 ML results indicate

the role of the moment orientation on the relative total supercell energies of SAMs. The total energy of Au(111) with a full monolayer of M9 is always lower than that of M1 with both the PBE and the optB86b-vdW functionals. On the other hand, M1 is more preferable than M9 in terms of stability since it always gives relatively stronger binding in both isolated and monolayer structures due to more favorable dipole-dipole interactions in SAMs.

The LDA tends to underestimate the adsorption energies because of improper description of the long-range correlations. PBE calculations favor a (5×5) film phase between the two competing surface structures since the dissociative adsorption energy per CT appears to be positive on $(\sqrt{19} \times \sqrt{19})R23.4^\circ$ structure. The inclusion of vdW interactions correct the average adsorption energy per CT of the latter phase to be slightly negative. Nevertheless, vdW-DF calculations still energetically prefer the (5×5) geometry. Therefore, the vdW corrections are important to get reasonable results for carboranethiol-metal systems.

Acknowledgements

This work was financially supported by TUBİTAK under grant no. 213M182. EM and GG also acknowledge partial support from Balıkesir University through BAP 2015/194.

References

- (1) Frasconi, M.; Mazzei, F.; Ferri, T. Protein immobilization at gold-thiol surfaces and potential for biosensing. *Anal. Bioanal. Chem.* **2010**, 398, 1545-1564.
- (2) Love, J. C.; Estroff, L. A.; Kriebel, J. K.; Nuzzo, R. G.; Whitesides, G. M. Self-assembled monolayers of thiolates on metals as a form of nanotechnology. *Chem. Rev.* **2005**, 105, 1103-1169.
- (3) Schreiber, F. Structure and growth of self-assembling monolayers. *Prog. Surf. Sci.* **2000**, 65, 151-256.

- (4) Vericat, C.; Vela, M. E.; Benitez, G.; Carro, P.; Salvarezza, R. C. Self-assembled monolayers of thiols and dithiols on gold: new challenges for a well-known system. *Chem. Soc. Rev.* **2010**, 39, 1805-1834.
- (5) Albayrak, E.; Karabuga, S.; Bracco, G.; Danisman, M. F. Investigation of the deposition and thermal behavior of striped phases of unsymmetric disulfide self-assembled monolayers on Au (111): The case of 11-hydroxyundecyl decyl disulfide. *J. Chem. Phys.* **2015**, 142, 014703.
- (6) Albayrak, E.; Karabuga, S.; Bracco, G.; Danisman, M. F. 11-Hydroxyundecyl octadecyl disulfide self-assembled monolayers on Au(111). *Appl. Surf. Sci.* **2014**, 311, 643-647.
- (7) Albayrak, E.; Danisman, M. F. Helium Diffraction Study of Low Coverage Phases of Mercaptoundecanol and Octadecanethiol Self-Assembled Monolayers on Au(111) Prepared by Supersonic Molecular Beam Deposition. *J. Phys. Chem. C* **2013**, 117, 9801-9811.
- (8) Grönbeck, H.; Curioni, A.; Andreoni, W. Thiols and Disulfides on the Au(111) Surface: The Headgroup-Gold Interaction. *J. Am. Chem. Soc.* **2000**, 122, 3839-3842.
- (9) Ferrighi, L.; Pan, Y.-X.; Grönbeck H.; Hammer, B. Study of Alkylthiolate Self-assembled Monolayers on Au(111) Using a Semilocal meta-GGA Density Functional. *J. Phys. Chem. C* **2012**, 116, 7374-7379.
- (10) Hayashi, T.; Morikawa, Y.; Nozoye, H. Adsorption state of dimethyl disulfide on Au(111): Evidence for adsorption as thiolate at the bridge site. *J. Chem. Phys.* **2001**, 114, 7615-7621.
- (11) Grönbeck, H.; Häkkinen, H.; Whetten, R. L. Gold-thiolate complexes form a unique $c(4 \times 2)$ structure on Au(111). *J. Phys. Chem. C* **2008**, 112, 15490-15492.
- (12) Grönbeck, H.; Häkkinen, H. Polymerization at the Alkylthiolate-Au(111) Interface. *J. Phys. Chem. B* **2007**, 111, 3325-3327.
- (13) Yourdshahyan, Y.; Rappe, A. M. Structure and energetics of alkanethiol adsorption on the Au(111) surface. *J. Chem. Phys.* **2002**, 117, 825-833.

- (14) Yourdshahyan, Y.; Zhang, H. K.; Rappe, A. M. *n*-alkyl thiol head-group interactions with the Au(111) surface. *Phys. Rev. B* **2001**, 63, 081405(R).
- (15) Vargas, M. C.; Giannozzi, P.; Selloni, A.; Scoles, G. Coverage-Dependent Adsorption of CH₃S and (CH₃S)₂ on Au(111): a Density Functional Theory Study. *J. Phys. Chem. B* **2001**, 105, 9509-9513.
- (16) Molina, L. M.; Hammer, B. Theoretical study of thiol-induced reconstructions on the Au(111) surface. *Chem. Phys. Lett.* **2002**, 360, 264-271.
- (17) Otálvaro, D.; Veening, T.; Brocks, G. Self-Assembled Monolayer Induced Au(111) and Ag(111) Reconstructions: Work Functions and Interface Dipole Formation. *J. Phys. Chem. C* **2012**, 116, 7826-7837.
- (18) Rusu, P. C.; Brocks, G. Surface Dipoles and Work Functions of Alkylthiolates and Fluorinated Alkylthiolates on Au(111). *J. Phys. Chem. B* **2006**, 110, 22628-22634.
- (19) Fertitta, E.; Voloshina, E.; Paulus, B. Adsorption of multivalent alkylthiols on Au(111) surface: insights from DFT. *J. Comput. Chem.* **2014**, 35, 204-213.
- (20) Abu-Husein, T.; Schuster, S.; Egger, D. A.; Kind, M.; Santowski, T.; Wiesner, A.; Chiechi, R.; Zojer, E.; Terfort, A.; Zharnikov, M. The Effects of Embedded Dipoles in Aromatic Self-Assembled Monolayers. *Adv. Funct. Mat.* **2015**, 25, 3943-3957.
- (21) Verwuester, E.; Hofmann, O. T.; Egger, D. A.; Zojer, E. Electronic Properties of Biphenylthiolates on Au(111): The Impact of Coverage Revisited. *J. Phys. Chem. C* **2015**, 119, 7817-7825.
- (22) Fajin, J. L. C.; Teixeira, F.; Gomes, J. R. B.; Cordeiro, M. N. D. S. Effect of van der Waals interactions in the DFT description of self-assembled monolayers of thiols on gold. *Theo. Chem. Acc.* **2015**, 134, 1-13.

- (23) Lustemberg, P. G.; Abufager, P. N.; Martiarena, M. L.; Busnengo, H. F. Adsorption of methanethiol on Au(1 1 1): Role of hydrogen bonds. *Chem. Phys. Lett.* **2014**, 610, 381-387.
- (24) Wang, Y.; Solano Canchaya, J. G.; Dong, W.; Alcamí, M.; Busnengo, H. F.; Martín, F. Chain-Length and Temperature Dependence of Self-Assembled Monolayers of Alkylthiolates on Au(111) and Ag(111) Surfaces. *J. Phys. Chem. A* **2014**, 118, 4138-4146.
- (25) Torres, E.; Blumenau, A. T.; Biedermann, P. U. Steric and chain length effects in the ($\sqrt{3} \times \sqrt{3}$)R30° structures of alkanethiol self-assembled monolayers on Au(111). *Chemphyschem* **2011**, 12, 999-1009.
- (26) Torres, E.; Blumenau, A. T.; Biedermann, P. U. Mechanism for phase transitions and vacancy island formation in alkylthiol/Au(111) self-assembled monolayers based on adatom and vacancy-induced reconstructions. *Phys. Rev. B* **2009**, 79, 075440.
- (27) Longo, G. S.; Bhattacharya, S. K.; Scandolo, S. A molecular dynamics study of the role of adatoms in SAMs of methylthiolate on Au(111): A new force field parameterized from ab initio calculations. *J. Phys. Chem. C* **2012**, 116, 14883-14891.
- (28) Cossaro, A.; Mazzarello, R.; Rousseau, R.; Casalis, L.; Verdini, A.; Kohlmeyer, A.; Floreano, L.; Scandolo, S.; Morgante, A.; Klein, M. L.; Scoles, G. X-ray Diffraction and Computation Yield the Structure of Alkanethiols on Gold(111). *Science* **2008**, 321, 943-946.
- (29) Mazzarello, R.; Cossaro, A.; Verdini, A.; Rousseau, R.; Casalis, L.; Danisman, M. F.; Floreano, L.; Scandolo, S.; Morgante, A.; Scoles, G. Structure of a CH₃S Monolayer on Au(111) Solved by the Interplay between Molecular Dynamics Calculations and Diffraction Measurements. *Phys. Rev. Lett.* **2007**, 98, 016102.
- (30) Rousseau, R.; De Renzi, V.; Mazzarello, R.; Marchetto, D.; Biagi, R.; Scandolo, S.; del Pennino, U. Interfacial Electrostatics of Self-Assembled Monolayers of Alkane Thiols on Au(111): Work Function Modification and Molecular Level Alignments. *J. Phys. Chem. B* **2006**, 110, 10862-10872.

- (31) De Renzi, V.; Rousseau, R.; Marchetto, D.; Biagi, R.; Scandolo S.; del Pennino, U. Metal Work-Function Changes Induced by Organic Adsorbates: A Combined Experimental and Theoretical Study. *Phys. Rev. Lett.* **2005**, 95, 046804.
- (32) Zhang, L. Z.; Goddard, W. A.; Jiang, S. Y. Molecular simulation study of the $c(4\times 2)$ superlattice structure of alkanethiol self-assembled monolayers on Au(111). *J. Chem. Phys.* **2002**, 117, 7342-7349.
- (33) Fischer, D.; Curioni, A.; Andreoni, W. Decanethiols on Gold: The Structure of Self-Assembled Monolayers Unraveled with Computer Simulations. *Langmuir* **2003**, 19, 3567-3571.
- (34) Osella, S.; Cornil, D.; Cornil, J. Work function modification of the (111) gold surface covered by long alkanethiol-based self-assembled monolayers. *Phys. Chem. Chem. Phys.* **2014**, 16, 2866-2873.
- (35) Barmparis, G. D.; Honkala, K.; Remediakis, I. N. Thiolate adsorption on Au(hkl) and equilibrium shape of large thiolate-covered gold nanoparticles. *J. Chem. Phys.* **2013**, 138, 064702.
- (36) Wang, J.-G.; Selloni, A. Influence of End Group and Surface Structure on the Current-Voltage Characteristics of Alkanethiol Monolayers on Au(111). *J. Phys. Chem. A* **2007**, 111, 12381-12385.
- (37) Wang, J.-G.; Selloni, A. The $c(4\times 2)$ Structure of Short- and Intermediate-Chain Length Alkanethiolate Monolayers on Au(111): A DFT Study. *J. Phys. Chem. C* **2007**, 111, 12149-12151.
- (38) Sun, Q.; Selloni, A. Interface and Molecular Electronic Structure vs Tunneling Characteristics of CH_3 - and CF_3 -Terminated Thiol Monolayers on Au(111). *J. Phys. Chem. A* **2006**, 110, 11396-11400.
- (39) De Renzi, V.; Di Felice, R.; Marchetto, D.; Biagi, R.; del Pennino U.; Selloni, A. Ordered (3×4) High-Density Phase of Methylthiolate on Au(111). *J. Phys. Chem. B* **2004**, 108, 16-20.

- (40) Heimel, G.; Romaner, L.; Zojer, E.; Bredas, J.-L. The Interface Energetics of Self-Assembled Monolayers on Metals. *Acc. Chem. Res.* **2008**, 41, 721-729.
- (41) Campbell, I. H.; Rubin, S.; Zawodzinski, T. A.; Kress, J. D.; Martin, R. L.; Smith, D. L.; Barashkov, N. N.; Ferraris, J. P. Controlling Schottky energy barriers in organic electronic devices using self-assembled monolayers. *Phys. Rev. B* **1996**, 54, 14321-14324.
- (42) Chen, C.-Y.; Wu, K.-Y.; Chao, Y.-C.; Zan, H.-W.; Meng, H.-F.; Tao, Y.-T. Concomitant tuning of metal work function and wetting property with mixed self-assembled monolayers. *Org. Elect.* **2011**, 12, 148-153.
- (43) Venkataraman, N. V.; Zuercher, S.; Rossi, A.; Lee, S.; Naujoks N.; Spencer, N. D. Spatial Tuning of the Metal Work Function by Means of Alkanethiol and Fluorinated Alkanethiol Gradients. *J. Phys. Chem. C* **2009**, 113, 5620-5628.
- (44) Alloway, D. M.; Graham, A. L.; Yang, X.; Mudalige, A.; Colorado Jr., R.; Wysocki, V. H.; Pemberton, J. E.; Lee, T. R.; Wysocki, R. J.; Armstrong, N. R. Tuning the Effective Work Function of Gold and Silver Using ω -Functionalized Alkanethiols: Varying Surface Composition through Dilution and Choice of Terminal Groups. *J. Phys. Chem. C* **2009**, 113, 20328-20334.
- (45) Wu, K.-Y.; Yu, S.-Y.; Tao, Y.-T. Continuous Modulation of Electrode Work Function with Mixed Self-Assembled Monolayers and Its Effect in Charge Injection. *Langmuir* **2009**, 25, 6232-6238.
- (46) Xu, Y.; Baeg, K.-J.; Park, W.-T.; Cho, A.; Choi, E.-Y.; Noh, Y.-Y. Regulating Charge Injection in Ambipolar Organic Field-Effect Transistors by Mixed Self-Assembled Monolayers. *ACS Appl. Mater. Interfaces* **2014**, 6, 14493-14499.
- (47) Lubben, J. F.; Base, T.; Rupper, P.; Kunniger, T.; Machacek, J.; Guimond, S. Tuning the surface potential of Ag surfaces by chemisorption of oppositely-oriented thiolated carborane dipoles. *J. Colloid Int. Sci.* **2011**, 354, 168-174.

- (48) Base, T.; Bastl, Z.; Havranek, V.; Lang, K.; Bould, J.; Londesborough, M. G. S.; Machacek, J.; Plesek, J. Carborane-thiol-silver interactions. A comparative study of the molecular protection of silver surfaces. *Surf. Coat. Tech.* **2010**, 204, 2639-2646.
- (49) Base, T.; Bastl, Z.; Plzak, Z.; Grygar, T.; Plesek, J.; Carr, M. J.; Malina, V.; Subrt, J.; Bohacek, J.; Vecernikova, E.; Kriz, O. Carboranethiol-Modified Gold Surfaces. A Study and Comparison of Modified Cluster and Flat Surfaces. *Langmuir* **2005**, 21, 7776-7785.
- (50) Base, T.; Bastl, Z.; Slouf, M.; Klementova, M.; Subrt, J.; Vetushka, A.; Ledinsky, M.; Fejfar, A.; Machacek, J.; Carr, M. J.; Londesborough, M. G. S. Gold Micrometer Crystals Modified with Carboranethiol Derivatives. *J. Phys. Chem. C* **2008**, 112, 14446-14455.
- (51) Scholz, F.; Nothofer, H. G.; Wessels, J. M.; Nelles, G.; von Wrochem, F.; Roy, S.; Chen, X. D.; Michl, J. Permethylated 12-Vertex *p*-Carborane Self-Assembled Monolayers. *J. Phys. Chem. C* **2011**, 115, 22998-23007.
- (52) von Wrochem, F.; Scholz, F.; Gao, D. Q.; Nothofer, H. G.; Yasuda, A.; Wessels, J. M.; Roy, S.; Chen, X. D.; Michl, J. High-Band-Gap Polycrystalline Monolayers of a 12-Vertex *p*-Carborane on Au(111). *J. Phys. Chem. Lett.* **2010**, 1, 3471-3477.
- (53) Kim, J.; Rim, Y. S.; Liu, Y.; Serino, A. C.; Thomas, J. C.; Chen, H.; Yang, Y.; Weiss, P. S. Interface Control in Organic Electronics Using Mixed Monolayers of Carboranethiol Isomers. *Nano Lett.* **2014**, 14, 2946-2951.
- (54) Hohman, J. N.; Claridge, S. A.; Kim, M.; Weiss, P. S. Cage molecules for self-assembly. *Mater. Sci. Eng. R-Rep.* **2010**, 70, 188-208.
- (55) Hohman, J. N.; Zhang, P.; Morin, E. I.; Han, P.; Kim, M.; Kurland, A. R.; McClanahan, P. D.; Balema V. P.; Weiss, P. S. Self-Assembly of Carboranethiol Isomers on Au111: Intermolecular Interactions Determined by Molecular Dipole Orientations. *ACS Nano* **2009**, 3, 527-536.

- (56) Bould, J.; Machacek, J.; Londesborough, M. G. S.; Macias, R.; Kennedy, J. D.; Bastl, Z.; Rupper, P.; Base, T. Decaborane Thiols as Building Blocks for Self-Assembled Monolayers on Metal Surfaces. *Inorg. Chem.* **2012**, 51, 1685-1694.
- (57) Thomas, J. C.; Schwartz, J. J.; Hohman, J. N.; Claridge, S. A.; Auluck, H. S.; Serino, A. C.; Spokoyny, A. M.; Tran, G.; Kelly, K. F.; Mirkin, C. A.; Gilles, J.; Osher, S. J.; Weiss, P. S. Defect-Tolerant Aligned Dipoles within Two-Dimensional Plastic Lattices. *ACS Nano* **2015**, 9, 4734-4742.
- (58) Thomas, J. C.; Boldog, I.; Auluck, H. S.; Bereciartua, P. J.; Dusek, M.; Machacek, J.; Bastl, Z.; Weiss, P. S.; Base, T. Self-Assembled *p*-Carborane Analogue of *p*-Mercaptobenzoic Acid on Au{111}. *Chem. Mater.* **2015**, 27, 5425-5435.
- (59) Blöchl, P. E. Projector Augmented-Wave Method. *Phys. Rev. B* **1994**, 50, 17953.
- (60) Kresse, G.; Hafner, J. Ab initio Molecular Dynamics for Liquid Metals. *Phys. Rev. B* **1993**, 47, 558.
- (61) Kresse, G.; Furthmüller, J. Efficient Iterative Schemes for Ab Initio Total-Energy Calculations Using a Plane-Wave Basis Set. *Phys. Rev. B* **1996**, 54, 11169.
- (62) Kresse, G.; Joubert, J. From Ultrasoft Pseudopotentials to the Projector Augmented-Wave Method. *Phys. Rev. B* **1999**, 59, 1758.
- (63) Klimeš, J.; Bowler, D. R.; Michaelides, A. Van der Waals Density Functionals Applied to Solids. *Phys. Rev. B* **2011**, 83, 195131.
- (64) Dion, M.; Rydberg, H.; Schröder, E.; Langreth, D. C.; Lundqvist, B. I. Van der Waals Density Functional for General Geometries. *Phys. Rev. Lett.* **2004**, 92, 246401.
- (65) Wyckhoff, R. G. "Crystal Structures", 2nd ed., Interscience Publishers, New York, 1958.